Reductive dimerization mechanisms of some streptocyanine dyes

Christiane André-Barrès, Fadia Najjar, Marie-Pierre Maether, Corinne Payrastre, Peter Winterton, Théodore Tzedakis

Reductive dimerization mechanisms of some streptocyanine dyes

Christiane André-Barrès [a,*], Fadia Najjar [a,b], Marie-Pierre Maether [a], Corinne Payrastre [a], Peter Winterton [c], Theo Tzedakis [d,*]

[a] Laboratoire de Synthèse et Physico-Chimie de Molécules d'Intérêt Biologique, CNRS UMR 5068, Université de Toulouse-UPS, 118, route de Narbonne, 31062 Toulouse, France
[b] Laboratoire de Chimie Organique Appliquée, Faculté des Sciences II, Université Libanaise, Département de Chimie et Biochimie, Jdeidit el Maten, P.O. Box: 90656, Liban
[c] Département Langues & Gestion, Université de Toulouse-UPS, 118, route de Narbonne, 31062 Toulouse, France
[d] Laboratoire de Génie Chimique, UMR 5503, Université de Toulouse-UPS, 118, route de Narbonne, 31062 Toulouse, France

ARTICLE INFO

ABSTRACT

Cyclic voltammetric studies of streptocyanine dyes were carried out on a glassy carbon electrode. For dye electroreduction, logarithmic analysis of the convoluted current indicates an EC2 mechanism with dimerization following electron transfer. Relevant kinetic and thermodynamic values are reported.

1. Introduction

Cyanine dyes are cationic conjugated organic compounds containing a polymethine chain with an odd number of carbon atoms between two nitrogen atoms. [1,2] Due to their photophysical properties they are used in numerous applications, such as photographic sensitizers, [3,4] infrared-dye-sensitized solar cells, [5] optical recording, [6] nonlinear frequency doublers, [7,8] or biological probes. [9–12] Cyanines are also known to possess interesting biological properties. [13] We previously described the synthesis and antimalarial properties of various polymethine chain lengths (5C, 7C and 9C) streptocyanine dyes (SD). [14] Electrochemical study of the redox behavior of three families of streptocyanines was considered here, using cyclic voltammetry to provide mechanistic information as well as physicochemical data on the compounds. Amatore and co-workers [15] uses electrochemical techniques to approach the biochemical mechanism of action of potential drug molecules on the redox machinery of the cells (NADPH-cytochrome P450 reductase). The authors state that the redox ability of these 'bio-reductive' drugs, expressed in terms of the redox potential, has to be in the range: $E_{activation\ by\ flavoproteines} < E_{'bio-reductive'\ drugs} < E_{protection\ against\ O2}$. The reduction potentials thus obtained must be in the range of -0.50 to -0.10 V vs. SHE in buffered aqueous media and more negative in non-aqueous media; the values calculated in [15] are: -1.10 to -0.70 V vs. SCE.

Note that the anti-cancer activity of both cyanine and merocyanine dyes has been correlated (patent [16]) with their redox potentials, particularly in the cathodic range from -1.10 to -0.80 V vs. SCE.

The present study, carried out using voltammetry techniques, focuses on both the anodic and cathodic electrochemical behaviors of various streptocyanine dyes. Resulting voltammograms were analyzed using deconvolution techniques, expecting to get a better understanding of their reductive reaction mechanism, especially regarding the evolution of the radicals produced by the cathodic reaction. Coupling of the data obtained here with the biological properties of streptocyanines should help to examine the

possibility to establish possible correlations between the electrochemical behavior of cyanines as well as their redox potential with their biological activity.

2. Experimental

Electrochemical experiments were performed using a previously described [17] three-electrode set-up with an Autolab PGSTAT 30. The medium was deaerated (Ar, 1 bar), acetonitrile containing 0.10 M tetrabutylammonium perchlorate (TBAP) and thermoregulated at 25 °C. The working electrode (3 mm diameter glassy carbon disk) was carefully polished, sonicated in 2-propanol for 10 min and finally dried in a stream of cool air. Before plotting the voltammograms, the electrode was activated by cycling several times from 2 to -2.5 V at 0.2 V.s^{-1}. The counter electrode was a 1 cm^2 platinum plate. A silver wire was used as pseudo-reference electrode; it was calibrated after each experiment against the ferrocene/ferricenium couple (0.475 V vs. SCE). A known concentration of ferrocene was added to the mixture studied and current potentials were plotted in the same conditions as for SD, in order to determine the potential of the position of the ferrocene oxidation peak. This potential is stable whatever the scan rate used, the uncertainty is + - 2 mV. Localization of the position of the ferrocene oxidation peak allowed the potentials of other signals to be determined versus the SCE. Impendence measurements allowed the determination of the ionic resistance of the mixture, and the value obtained was applied (feedback correction) to compensate for the ohmic drop between the working and reference electrodes.

The syntheses of 5C-, 7C-, 9C- streptocyanine dyes and of 5C-hemicarboxonium studied in the present work (Fig. 1), have been reported previously. [18–21]

3. Theoretical part

Cathodic reduction of streptocyanine dyes leads to a radical (shown a one electron cathodic peak, reaction 1), which can be involved in followed chemical reaction (2). This voltammetric study, expects to get a better understanding of their overall process of SD reduction, especially regarding the evolution of the radicals produced by the cathodic reaction. Especially, this section focuses on the kinetics of the process and especially on chemical reaction (2) which is linked to electron transfer (1).

$$SD^+ + e^- \xrightarrow{k_{ET}} SD^\circ \tag{1}$$

$$pSD^\circ \xrightarrow{k_\chi} products \tag{2}$$
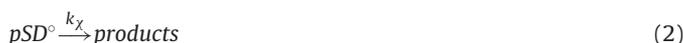
Limitation of the kinetics of the overall process could be due to: -the electron transfer (1), -the chemical reaction (2), -the diffusion process; mixed character limitation could also be observed.

To achieve this goal, the influence of the potential scan rate, r, on both the peak potential (E_p) and the difference $|E_{pc}$-$E_{pc/2}|$ was examined: these parameters can provide information on the limiting step of the overall process. Formal kinetics have been largely described by Savéant and co-workers [22,23] and the values of the two most significant parameters ($|E_{pc}$-$E_{pc/2}|$ and $\frac{\partial E_p}{\partial \log r}$) are indicated in the two extreme cases in Table 1.

3.1. Convolution potential sweep voltammetry assignments

Experimentally obtained voltammograms (see section 4) were analyzed using the convolution potential sweep voltammetry method [24]. The convoluted current $I(t)$ is related to the actual current $i(t)$ through the convolution integral:

$$I(t) = \frac{1}{\pi^{1/2}} \int_0^t \frac{i(u)}{(t-u)^{1/2}} du \tag{3}$$

The convoluted limiting value of $I(t)$, solely controlled by the diffusion flux at the electrode, is expressed by:

$$I_{lim} = n \times F \times S \times c^\circ \times D^{1/2} \tag{4}$$

where n is the electron exchanged, S is the electrode area, D is the diffusion coefficient, c° is the concentration of the streptocyanine.

The potential of the cathode can be expressed as a function of both the convoluted and the actual current, as well as the chemical rate constant k_χ according to the limitation (chemical or electrochemical).

-low rate constant k_χ for the chemical reaction (2):

The overall system is in pure diffusion control (the influence of the chemical reaction is negligible with charge transfer remaining Nernstian). The following equations allow the potential of the cathode to be determined:

$$E = E^\circ + \frac{RT}{F} \ln \frac{[I_{lim} - I]}{I} \tag{5}$$

$$\left| E_p - E_{p/2} \right| = 2.20 \frac{RT}{F} = 57.5 mV \tag{6}$$

$$\frac{\partial E_p}{\partial \log r} = 0 \tag{7}$$

-high rate constant k_χ for the chemical reaction (2):

The overall kinetics of the system is influenced by the chemical reaction (pure kinetic conditions). The cathode potential
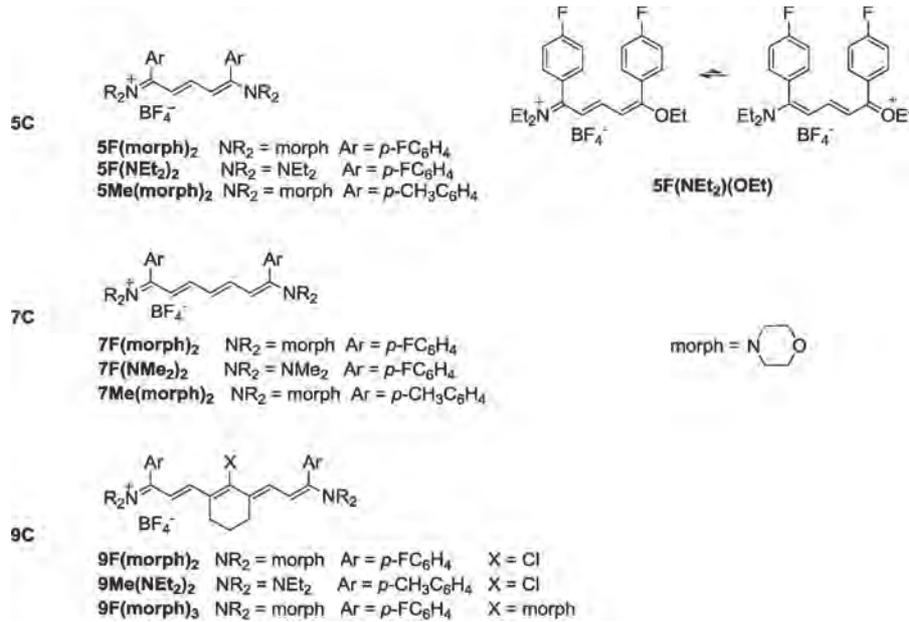
Fig. 1. Structures of 5C, 7C and 9C streptocyanine dyes and 5C-hemicarboxonium.

can be expressed by equation (8) if the chemical reaction is a rearrangement [25] with a chemical rate of $k_\chi^*[SD^\circ]^1$, or by equation (9) in the case of a dimerization [26] with a chemical rate of $k_\chi^*[SD^\circ]^2$.

$$E = E^\circ + \frac{RT}{2F} \ln k_\chi + \frac{RT}{F} \ln \frac{[I_{lim} - I]}{i} \qquad (8)$$

$$E = E^\circ + \frac{RT}{3F} \ln \frac{2k\chi c^\circ}{3I_{lim}} + \frac{RT}{F} \ln \frac{[I_{lim} - I]}{i^{2/3}} \qquad (9)$$

Note that in second order chemical reactions the response of the system can be expressed by the dimensionless parameter [23,26] $\lambda = (RT/F)(k_\chi c^\circ / r)$ with $\log \lambda \geq 0.13$ in the pure kinetic zone.

Moreover, for kinetic control (high rate constant k_χ) of the overall process (reactions 1 and 2), the convolution potential sweep voltammetry method [27,28] shows that:

- the electron transfer constant k_{ET} can be linked to the convoluted current according to (10),

$$\ln k_{ET}(E) = \ln D^{1/2} - \ln \left[(I_{lim} - I)/i \right] \qquad (10)$$

- the cathodic transfer coefficient (α) dependence with the potential can be expressed by (11)

$$\alpha = \frac{\partial \Delta G^{\#}}{\partial \Delta G^0} = 0.5 + \frac{F(E - E^0)}{8 \Delta G_0^{\#}} = \frac{-RT}{F} \frac{d \ln k_{ET}}{dE} \qquad (11)$$

The potential versus the logarithm of the corresponding function of the convoluted current (equations 5, or 8 or 9) gives the corresponding limitation of the overall process e.g. the different zones of diffusion or kinetic control (by the chemical reaction). Note that a nonlinear variation of E versus the appropriate function in the previous equations, translates mixed limitation zones.

Various kinds, described below, can be observed:

*The electrode potential, varies linearly versus $\ln[(I_{lim}-I)/I]$ (equation 5), and the slope of the plot is consistent with the theoretical value of 25.6 mV. This behavior, especially observed for high potential scan rates (> ~3 V/s) minimizes the effect of the chemical reaction (2), means that the overall SD reduction process is under diffusion control. The intercept of the plot provides E°. Note that E° can also be estimated from the arithmetic mean of anodic and cathodic peak potentials $E^\circ = (E_{pa} + E_{pc})/2$ at high scan rates.

** The linearity between the electrode potential and the logarithmic function of the current (equations (8) and (9)), can be observed for lower potential scan rates (< ~1 V/s). For the SD in question, this behavior means that the overall reduction process is under pure kinetic control by chemical reaction (2)–its order being determined experimentally.

Absence of linearity for plots (5), (8) or (9), translates mixed limitation, e.g. similar magnitude of electron transfer and chemical reaction rates.

4. Experimental results and discussion

Voltammograms were recorded for various SD (5 C, 7 C and 9 C), in the potential range from -2.5 to 2 V, at various potential scan rates (0.1 to 5 V.s^{-1}), nevertheless for simplicity of reading only voltammograms, obtained at 0.6 V.s^{-1}, are shown in Fig. 2.

Curves for each SD were first (Fig. 2, curves 1) plotted starting at oxidation, and a complete cycle $E_{i=0} \rightarrow 2 V \rightarrow -2.5 V \rightarrow E_{i=0}$ was performed.

In a second time, curves were plotted for the same SD starting in the cathodic direction

Table 1
Values of parameters ($|E_p$-$E_{p/2}|$ and $\frac{\partial E_p}{\partial \log r}$), in the two extreme cases, from Savéant and co-workers. [22,23].

	The chemical reaction following the electron transfer is slow and controls the overall kinetics		The electron transfer controls the overall kinetics, which can follow a concerted or stepwise mechanism	
	$\left|E_p - E_{p/2}\right|$ (mV)	$\frac{\partial E_p}{\partial \log r}$ (mV/decade of r)	$\left|E_p - E_{p/2}\right|$ (mV)	$\frac{\partial E_p}{\partial \log r}$ (mV/decade of r)
1st order chemical reaction	$1.857 \frac{RT}{nF} = \frac{47.5}{n}$	$-\frac{RT}{2nF} \ln 10 = -\frac{29.6}{n}$	$\frac{47.5}{\alpha n}$	$-\frac{29.6}{\alpha n}$
2nd order chemical reaction (e.g. dimerization)	$1.512 \frac{RT}{nF} = \frac{38.8}{n}$	$-\frac{RT}{3nF} \ln 10 = -\frac{19.7}{n}$	$\frac{38.8}{\alpha n}$	$-\frac{19.7}{\alpha n}$

Fig. 2. a Voltammetric curves plotted at 0.6 V.s-1 on glassy carbon disk shaped cathode, with streptocyanines 5F(morph)2 and 5F(NEt2)2 and hemicarboxonium 5F(NEt2)OEt at 1 mM into acetonitrile and in presence of TBAP. Residual current was removed and the potential is calibrated against the comparison electrode previously described. Curves (1): forward scan to the positive direction; Curves (2): forward scan to the negative direction. Fig. 2b same caption as Fig. 2a for 7F(NEt2)2, 7F(morph)2 and 9F(morph)2, 9Me(NEt2)2.

($E_{i=0} \rightarrow -2.5\,V \rightarrow 2\,V \rightarrow E_{i=0}$ (Fig. 2, curves 2)). The operating mode allows:i) the independent study of the nature of each anodic or cathodic signal, ii) to show if observed signals in the first run were present in the second one, iii) to show if for example the first oxidative step irreversibly modify the signals observed in the cathodic area or not, e.g. if these signals correspond to the same groups transformed or to different groups, and vice versa.

Compound	E_{p1a}	$E°$	E_{p1c}
5F(NEt$_2$)$_2$	-	1.16	-1.15
5F(morph)2	-	1.19	-0.89
5Me(morph)2*	-	1.15	-0.97
5F(NEt2)(OEt)	1.66	nd	-0.80
7F(NMe2)2	0.74	nd	-0.88
7F(morph)2	0.83	nd	-0.68
7Me(morph)2*	0.80	nd	-0.75
9Me(NEt2)2	0.42	0.37	-0.94
9F(morph)2	0.65	0.61	-0.50
9F(morph)3 (fig. 3)	0.68	0.59	-0.81

*Curves presented in supplementary material

4.1. Qualitative analysis of voltammetric curves obtained starting in oxidation

Starting in oxidation, curves 1 (Fig. 2) obtained with the 5F(Morph)$_2$ or 5F(NEt$_2$)$_2$ exhibit an anodic peak at ~1.3 V, the backward curve contains the corresponding cathodic peak at ~1.2 V, and the overall redox system appears to be reversible. The $E°$ of this corresponding redox system is indicated in Table 2. Note that, if the scan starts to the cathodic direction (curves 2, Fig. 2), this reversible signal (both anodic and cathodic peaks) is present at the same potential values, indicating that the corresponding group was not affected when the reduction of the 5F(Morph)$_2$ or 5F(NEt$_2$)$_2$ is first achieved.

For all other compounds studied, curves show significant differences when compared against the systems 5F(Morph)$_2$ or 5F(NEt$_2$)$_2$; indeed:

i) 5F(NEt$_2$)(OEt), and 7 C SD present irreversible anodic peak.
ii) For the 9 C SD, two peaks appear in oxidation, the first seems to be partially reversible (Q_{anodic} ~3 × $Q_{cathodic}$); the second, located at higher potential, appears to be totally irreversible.
iii) Increasing the length of the carbon chain (from 5 to 9), allows easier oxidation of streptocyanines; indeed going from 5 C to 9 C, anodic peak potential decreased from ~1.3 V (anodic signal for 5 C) to ~ 0.4 V (first anodic signal for 9 C). The main reason explaining the decreases of the peak potential against the carbon chain length is the greater delocalization, allowing easier

electron removal, as indicated in Scheme 1 for the corresponding SD. The stabilization of the dicationic radical produced at the electrode can be explained by the analysis of limit forms. Electron spin density is localized on even carbons and to a lesser extent on the heteroatom N or O.

The dicationic radical is persistent in the case of 5 C due to charge repulsion in the vicinity of the radical preventing its dimerization. Conversely, an irreversible system at higher potential (1.7 V) is observed in the case of the hemicarboxonium 5F(NEt$_2$)(OEt). Note that delocalization is less pronounced as the charge is localized on the nitrogen and not on the whole chain as for the streptocyanines. So, removal of one electron is more difficult.

Concerning the 7C-SD, one limit form is preponderant because of symmetry, with spin density localized on carbon 4, and radical more distant of charges consequently more reactive, and so giving an irreversible peak in cyclic voltammetry.

Concerning the 9C-SD, several limit forms are present with a tertiary radical on position 4 or 6, explaining the persistency of the dicationic radical observed in this series.

iv) Comparison of the curves (fig. 2, curves 1), does not show an effect of the amino groups located at the end of the carbon chains, on the peak potentials.

4.2. Qualitative analysis of voltammetric curves obtained starting in reduction

Starting in reduction (curves 2, fig. 2,), curves obtained with all examined compounds, exhibit a cathodic irreversible peak (E_{pc}) at the potential ranges from -1 to -0.4 V. Significant changes in the peak potential E_{pc} were observed as a function of the lateral groups of the compounds, as well as the C chain length:

i) Increasing the length of the carbon chain (from 5 to 9), allows easier reduction of SD; indeed going from SD-5 C to SD-9 C, increases the peak potential of the cathodic signal. For example, for SD containing the morpholine group: E_{pc}(SD-5 C) = - 0.89 V < E_{pc}(SD-7 C) = -0.68 V < E_{pc}(SD-9 C) = -0.50 V.
ii) For SD molecules containing the same number of carbon atoms, reduction is more difficult if the amino group of SD is -NMe$_2$ or -NEt$_2$ than the morpholine group. For SD-5 C family, reduction facility decreases
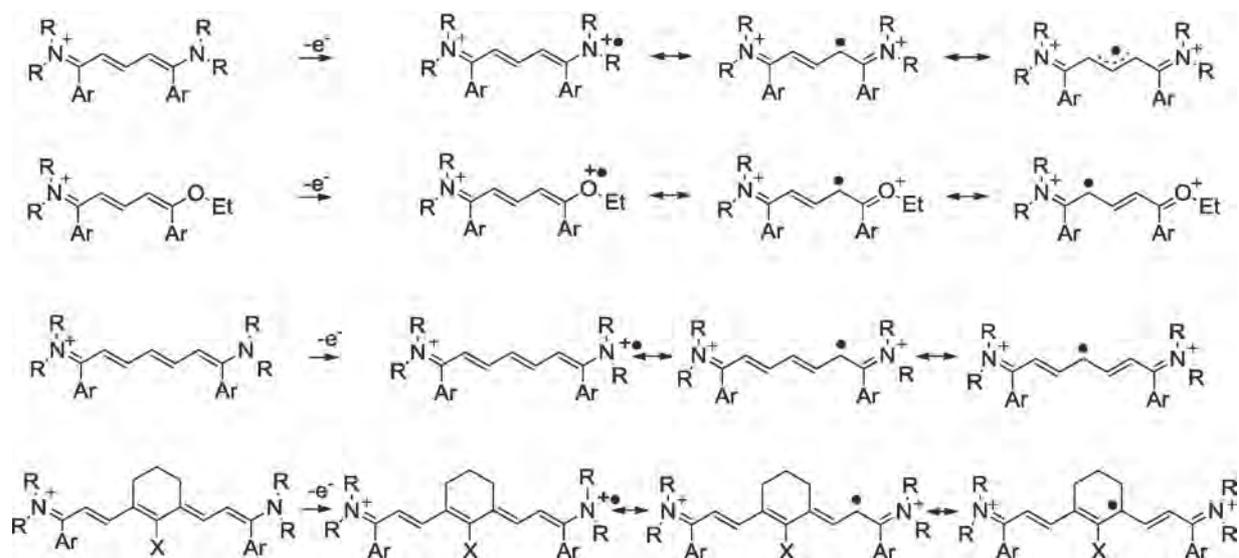
Scheme 1. Mechanism expected of the oxidation of 5C, 7C and 9C cyanines dyes and the hemicarboxonium, to the corresponding dicationic radical species: electron spin density is localized on even carbons.
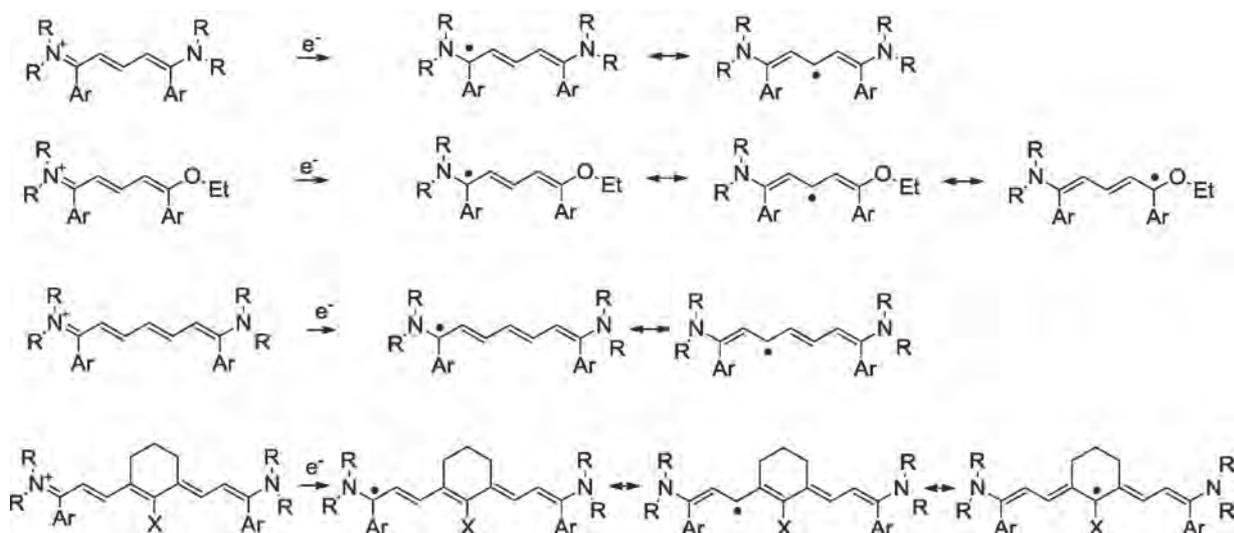
Scheme 2. ReSduction of 5C, 7C and 9C cyanines dyes to the corresponding neutral radical species: electron density is localized on odd carbons.
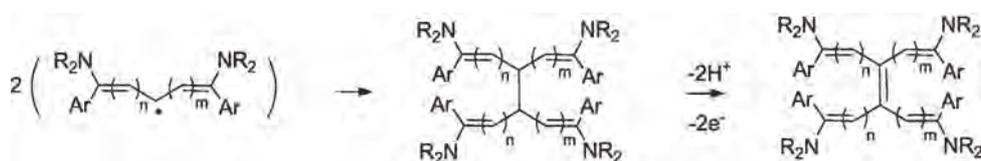
Scheme 3. Dimerization of neutral radical followed by oxidation.

according the following order: $E_{pc}(5F(NEt_2)(OEt)) \sim -0.80$ V $> E_{pc}(5F(morph)_2) \sim -0.89$ V $> E_{pc}(5F(NEt_2)_2) \sim -1.15$ V.

This evolution could be explained by the fact that the amino groups (NMe_2 or NEt_2) are more basic than the morpholine group with 2 log units, making reduction more difficult. [29] The presence of electro-withdrawing group as the fluorine in the *para* position on the ring facilitates the reduction. For 5F(NEt_2)(OEt), the positive charge is localized on nitrogen allowing its easier reduction (instead of a greater conjugation for other SD, as indicated in Scheme 2; Scheme 2 presents the expected mechanism of the reduction of SD (5 C, 7 C and 9 C) and the 5 C hemicarboxonium to the corresponding neutral radical species.

iii) As reduction leads to neutral radical, dimerization is straightforward as there is no charge repulsion, and could produce a polyconjugated dye as described in Scheme 3. Note that several isomers (mixture of Z and E double bond) and/or diastereoisomers could be obtained after the dimerization, that explain the lower magnitude peaks/waves, appearing in the backward (anodic) scan in the range of -0.2 V to -1 V. These new generated signals are due to the oxidation of these different isomers or diastereoisomers following the mechanism presented in Scheme 3.

iv) As previous (4-1/) if the scan starts to the anodic direction (curves 1, Fig. 2), the irreversible cathodic peak (E_{pc}) is present at the same potential values (-1 to -0.4 V), indicating that the corresponding group was not affected during oxidation.

4.3. Qualitative analysis of the voltammetric curves obtained with SD-9F(morph)₃

SD-9F(morph)₃, containing three morph groups, exhibited two reversible behavior signals in the potential range from -0.6 to +0.6 V (Fig. 3). (a-thin line): forward scan in the cathodic direction; (b-thin line): forward scan in the anodic direction; (c-thick line): forward

scan to cathodic direction to -0.9 V and return to anodic direction to +0.9 V.

These signals were obtained irrespective of the direction of the scan (curves (a), (b) or complete cycles (c)). Their standard potentials were respectively $E° = 0.59$ V ($\Delta E_{pc}-E_{pa} = 58$ mV) for the anodic curve, and $E° = -0.72$ V ($\Delta E_{pc}-E_{pa} = 70$ mV) for the cathodic curve. This reversibility can be explained by the persistency of the delocalized dicationic radical produced at the anode and the preponderance of the tertiary dicationic radical on carbons 4 and 6; the neutral radical appearing at the cathode has a preponderant limit form on carbon 5 and is stabilized by the morpholine-group.
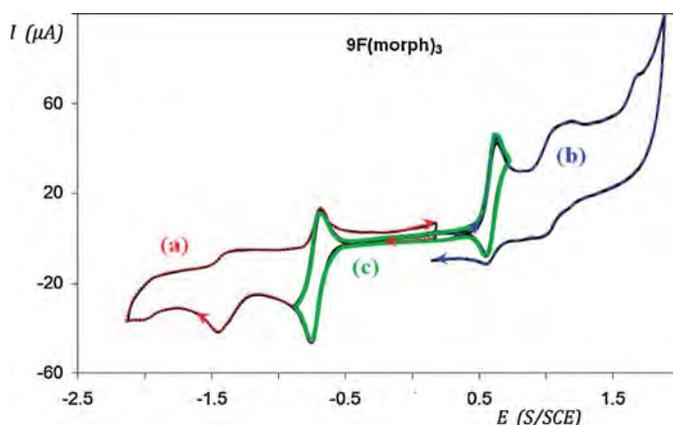
Fig. 3. Voltammetric curves plotted on glassy carbon disk shaped electrode, with 9F(morph)3 streptocyanine at 1 mM in acetonitrile and in the presence of TBAP. Residual current was removed and the potential calibrated against the comparison electrode as previously described; potential scan rate 0.6 V.s-1. Curves: (a-thin line) forward scan in the cathodic direction; (b-thin line): forward scan in the anodic direction; (c-thick line): forward scan to cathodic direction to -0.9 V and return to anodic direction to +0.9 V.
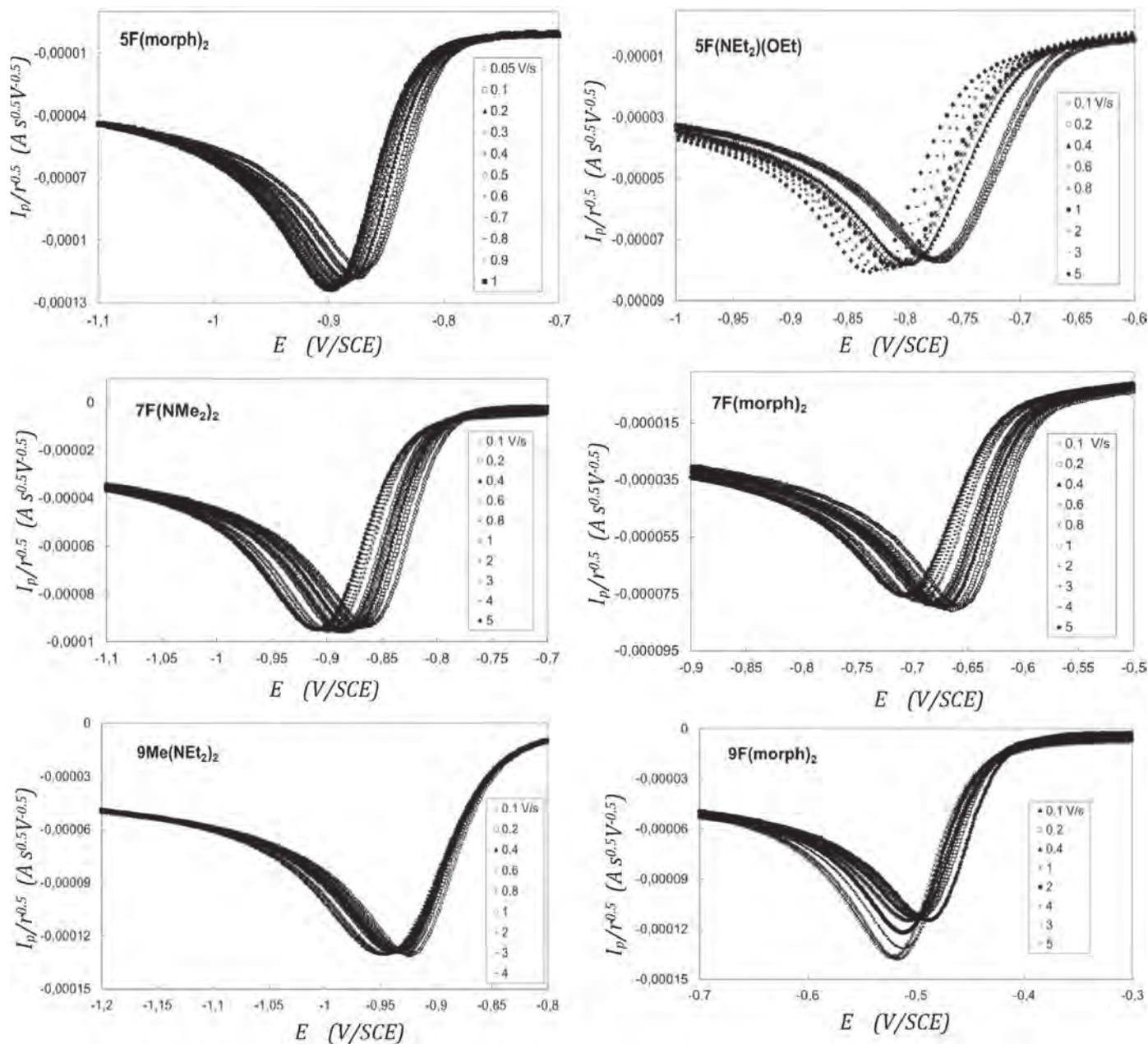
Fig. 4. Normalized current against the potential at different scan rate (r is in the range 0.1 to 5 V/s) for the various examined compounds.

4.4. Quantitative analysis of the cathodic part of the voltammetric curves

4.4.1. Potential scan rate dependence on the peak potential and current of the reduction of SD

Standard redox potentials $E°$ and anodic and cathodic peak potentials E_{pa}, E_{pc} determined by cyclic voltammetry measurements for the examined SD (curves of Figs. 2 and 3) are summarized in Table 2.

The curves of the normalized current $i_p/r^{1/2}$ (of the cathodic irreversible signal located in the potential range of -1.2 to -0.5 V (curves of Fig. 2)) against the potential, at different scan rate were presented in Fig. 4. Analysis of the normalized current, against the square root of the potential scan rate, does not indicate a constant evolution in the whole examined range of the potential scan rate. Depending on the compounds examined, the straight line

obtained can increase or decrease at higher potential scan rates. This nonlinear evolution of $I_{peak}/r^{0.5} = f(r^{0.5})$ (positive or negative dependence) confirms that there is a chemical reaction following the electron transfer probably a dimerization according an EC2 mechanism.

Table 3 Here On the other hand, analysis of the experimental results shows that for each streptocyanine, the peak potential (E_p) varies linearly versus the logarithm of the potential scan rate. The values of the slopes ($-\partial E_p/\partial \log r$) and the peak width | E_{pc}-$E_{pc/2}$| (summarized in Table 3) were found respectively in the range of 14/35 mV/decade of r and 37/52 mV following the SD and are presented in supplementary material.

Analysis of these parameters for most of the SD examined indicates rapid electron transfer and limitation of the overall cathodic process caused by a chemical reaction (2) (probably dimerization of the radical produced) [30].

Table 3
Kinetic and thermodynamic values obtained for reduction for SD and hemicarboxonium.

Compounds	Ep1c (V) (at 0.6 V.s^{-1})	$-\partial Ep/\partial logr$ mV/decade of r	r(V.s^{-1})	|Ep1c-Ep1c/2| (mV)	(10^3 k_χ) (M-1.s^{-1})	kET (cm s^{-1})	logλ; (r) (in V.s^{-1})	E (V)
5F(morph)$_2$	-0.89	24	0.10	37	66	-	-	-
			1.00	41			0.19; (1)	-
			5.00	nd			-	-0.87
5F(NEt$_2$)$_2$	-1.15	21	0.10	40	6	-	0.22; (0.1)	-
			1.00	42			-	-
			5.00	47			-	-1.12
5F(NEt$_2$)(OEt)	-0.80	32	0.10	57	-	-	-	-
			1.00	52			-	-0.88
			5.00	48			-	-0.78
7F(morph)$_2$	-0.68	30	0.10	40	-	0.10	-	-
			1.00	45			-	-
			5.00	50			-	-0.72
7F(NMe$_2$)$_2$	-0.88	22	0.10	39	64	-	-	-
			1.00	44			0.25; (1)	-
			5.00	47			-	-0.86
9F(morph)$_2$	-0.50	19	0.10	37	24	-	-	-
			1.00	41			0.21; (0.6)	-
			5.00	43			-	-0.48
9Me(NEt$_2$)$_2$	-0.94	14	0.05	nd	< 5	-	-	-
			0.10	43			-	-
			1.00	52			-	-
			5.00	58			-	-0.91

### 4.4.2. Kinetics of reaction (2) following the electron transfer

4.4.2.1. Study of the 5F(morph)$_2$, 5F(NEt$_2$)$_2$, 7F(NMe$_2$)$_2$, and 9F(morph)$_2$ at low scan rates (< 1 V/s). The logarithmic analysis of the convoluted current versus the potential, (according equation 9, deduced for a second order chemical reaction), gave a good correlation (Table 3 and Fig. 5) for the following streptocyanines 5F(morph)$_2$, 5F(NEt$_2$)$_2$, 7F(NMe$_2$)$_2$, and 9F(morph)$_2$.

*For 5F(morph)$_2$, the correlation obtained {E =0.026× ln[(I_{lim}-I)/$i^{2/3}$] - 0.75}, coupled with the assumed value of $E° = (E_{pa} + E_{pc})/2$ = -0.87 V at 1 V.s^{-1}, gives the second order rate constant of the chemical step $k_\chi = 6.0 \times 10^4$ L.mol^{-1} s^{-1} from the intercept value. The dimensionless parameter [23–26] $\lambda = (RT/F)(k_\chi c°/r)$ was found to be equal to 1·209, indicating limitation from the chemical reaction.

*In 5F(NEt$_2$)$_2$, the correlation obtained was $E = 0.0275 \times$ ln[(I_{lim}-I)/$i^{2/3}$]−0.998 (for $r \leq 0.2$ V.s^{-1}). Along with the standard potential of the system (determined below), it can be used to calculate $k_\chi = 6 \times 10^3$ L.mol^{-1}.s^{-1} and $\lambda = 1.246$, leading to the same conclusion as before.

*Operating in similar way for 7F(NMe$_2$)$_2$, using both the correlation obtained and $E = 0.0253 \times$ ln[(I_{lim}-I)/$i^{2/3}$]-0.738 and the standard potential of the system (determined below), $k_\chi = 6.4 \times 10^4$ L.mol^{-1}.s^{-1} and $\lambda = 1.284$ are obtained.
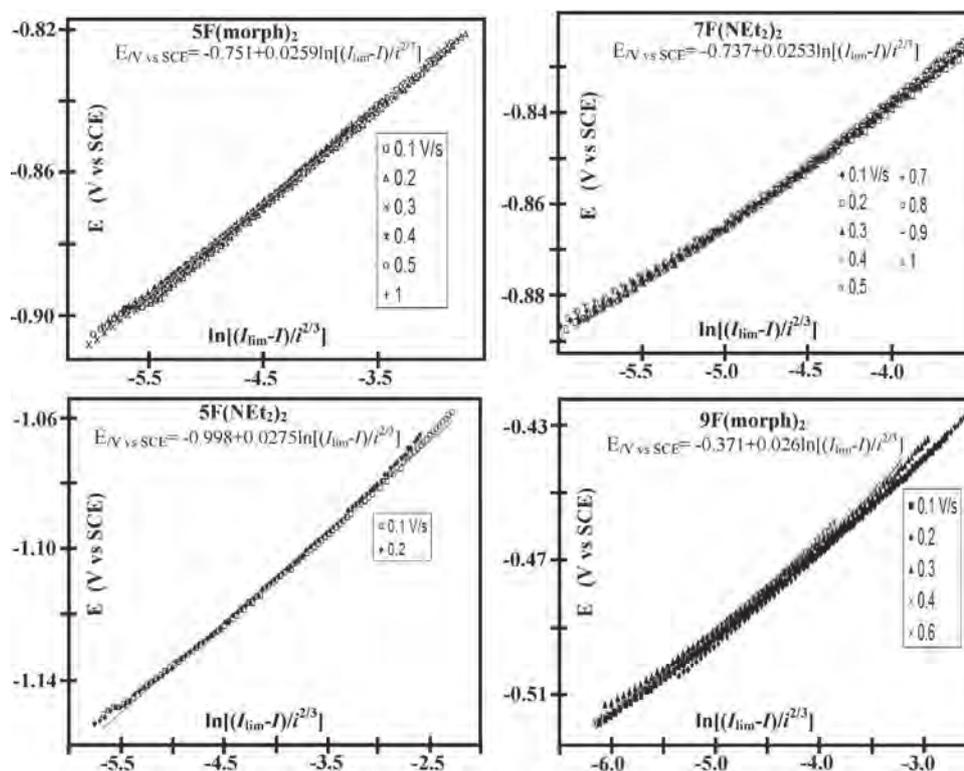
Fig. 5. Potential dependence of the convoluted current for 5F(morph)2, 5F(NEt2)2, 7F(NMe2)2 and 9F(morph)2. Potential scan rates in the range of 0.1 to 1 V/s.
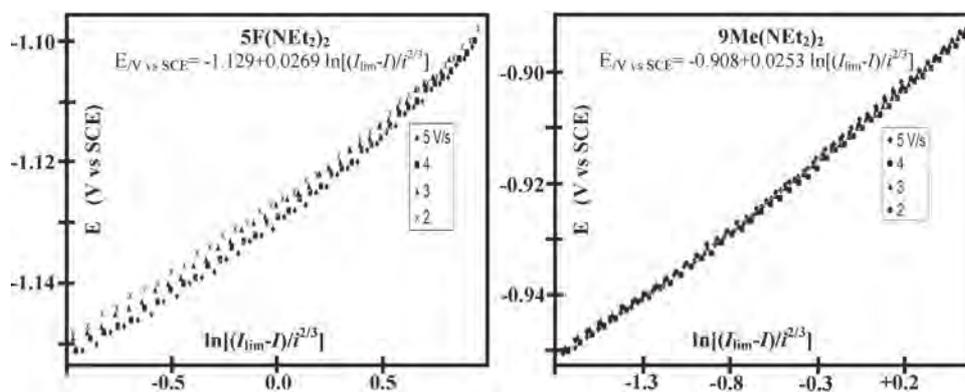
Fig. 6. Potential dependence of the convoluted current for 5F(NEt2)2, 9Me(NEt2)2. Involved potential scan rates in the range of 2 to 5 V/s

*Finally, for 9F(morph)$_2$ following correlation $E = 0.026 \times \ln[(I_{lim}-I)/i^{2/3}]$ -0.371 leads to $k_\chi = 2.4 \times 10^4$ L.mol^{-1}.s^{-1} and $\lambda = 1.234$ at $r = 0.6$ V.s^{-1}.

*Note that for 9Me(NEt$_2$)$_2$ a nonlinear correlation was obtained (not represented), meaning that the kinetic control by dimerization reaction (2) was not reached even at scan rates as low as 0.1 V/s.

To sum up, the kinetic rate constant was found to be of the same magnitude (10^{+4}) for all streptocyanines studied, except for 5F(NEt$_2$)$_2$ which exhibited a ~10-fold lower value.

4.4.2.2. Study of the 5F(NEt$_2$)$_2$ and 9Me(NMe$_2$)$_2$, at higher scan rates ($r \geq 3$ V.s^{-1}).

The logarithmic analysis of the convoluted current versus the potential, (according equation 5, verified for more rapid scan than in 4-4-2-1), deduced for an electron transfer limitation gives the standard potentials of streptocyanines 5F(NEt$_2$)$_2$ and 9F(morph)$_2$ (Table 3 and Fig. 6).

*Analysis according to (eq 5) led, for 5F(NEt$_2$)$_2$ to: E =0.026 × ln[(I_{lim}-I)/I] - 1.126, a correlation for which the intercept directly gives an estimation of $E° = -1.126$ V. Total reversibility was reached for scan rates higher than 5 V.s^{-1}, allows the peak potentials give a standard potential estimation of $E° = (E_{pa}+E_{pc})/2 = -1.120$ V, a value in good agreement with the previous one.

*Conversely, 9Me(NEt$_2$)$_2$ curve analysis according to (eq 5) led to linearity ($E = 0.0253 \times$ ln[(I_{lim}-I)/I] - 0.91) in a larger range of potential scan rates ($0.6 \leq r/$V.s$^{-1} \leq 5$, Fig. 6), and the standard potential deduced from the intercept is -0.91 V. The system, exhibiting pure diffusion control at scan rates ≥ 5 V/s (Table 3), became reversible, allows determinations of $|E_{pc}-E_{pc/2}| = 58$ mV and $(E_{pa}+E_{pc})/2 = E° = -0.92$ V, results in agreement with those estimated above.

*Note that for 9F(morph)$_2$, (curves not represented here) reversibility appears at 4 V s^{-1}. Its standard potential, determined at 5 V.s^{-1} is $(E_{pa}+E_{pc})/2 = E° = -0.484$ V.

*Intermediate behavior was observed for 7F(NMe$_2$)$_2$; indeed analysis with (eq 5) did not provide linear correlation even at high scan rates. Pure diffusion zone was not reached at 5 V.s^{-1}, but partial reversibility appeared at scan rates higher than 3 V.s^{-1} giving a rough estimation of $E°$ from the peak potentials: $E° = (E_{pa}+E_{pc})/2 = -0.860$ V.

To summarize, at low scan rates ($r \leq 0.2$ V.s^{-1}) the overall kinetics was controlled by the second order chemical reaction (2), for all SD examined (except 9Me(NEt$_2$)$_2$).

Increases the scan rate (0.4 to 1 V.s^{-1}) shown competition between reaction (1) e.g. Nernstian charge transfer and chemical reaction (2) e.g. dimerization for some SD (fig. 5). No simple log analysis was available in this zone.

Total reversibility was reached at scan rates higher than 5 V.s^{-1} for all SD examined, except for 7F(NMe$_2$)$_2$.

4.4.3. Kinetics of the electron transfer reaction (1) preceding the chemical reaction

7F(morph)$_2$ exhibits a specific behavior: slope $-\partial E_p/\partial \log r = 30$ mV/decade, and $|E_p$-$E_{p/2}|$ was found to increase from 40 to 50 mV as the sweep rate increased from 0.1 to 5 V.s^{-1}.

Neither equations (9) nor (5) led to a linear correlation in the potential scan rates in the range 0.1-5 V.s^{-1}.

For reduction process governed by electron transfer (followed by fast dimerization), the apparent cathodic transfer coefficient α_{ap} could be evaluated from equations (12) and (13)[27], at 0.65 and 0.78 respectively.

$$\alpha_{ap} = -19.7/(\partial E_p/\partial \log r) \tag{12}$$

and

$$\alpha_{ap} = 38.8/|E_p-E_{p/2}| \tag{13}$$

Based on the Marcus theory, the dependence of the cathodic transfer coefficient on the potential can be reached (for $r > 0.1$ V.s^{-1}) by a combination of equations (10) and (11), and using a value of 1.3×10^{-9} m^2.s^{-1} for D [31] (Fig. 7). At $\alpha = 0.5$, $E° = -0.72$ V and $k_{ET} = 0.1$ cm.s^{-1}. The overall kinetics is controlled by electron transfer for $r \geq 0.4$ V s^{-1}, by a stepwise mechanism ($\alpha > 0.5$).

-The mechanism is different in the case of this hemicarboxonium 5F(NEt$_2$)OEt where the conjugated system is less delocalized. Slope $\partial E_p/\partial \log r$ is -32 mV/decade of r, and the peak width ($|E_p$-$E_{p/2}| = 57$ mV at 0.1 V.s^{-1}) decreases for increasing scan rates. Analysis with equation (8 e.g. a first order chemical reaction following electron transfer) does not provide a linear evolution of ln[(I_{lim}-I)/i] versus E, excluding kinetic limitation. If the kinetics is governed by electron transfer, followed by fast dimerization, the apparent transfer coefficient α_{ap} can be evaluated from equations (12) and (13), respectively at 0.60 and 0.68. Variation of log k_{ET} with potential (combination of (10), (11) and $D = 1.5 \times 10^{-9}$ m^2.s^{-1} [31]) was not linear (Fig. 7) thus indicating that the classical Butler-Volmer equation is not applicable in this case (0.1–5 V.s^{-1}). Consequently, the quadratic activation-driving force relation (11) arising from the Marcus theory was employed to evaluate α by derivatization of lnk_{ET} (E). The data were derivatized in steps of 15 mV yielding the parabolic-shaped curve depicted in Fig. 7. Interestingly, the variation of α with E presents two linear regions implying two different reductions. This behavior is generally observed when the mechanism of the reduction changes from 'stepwise' to 'concerted'. Two standard reduction potentials ($E°$) could be evaluated (at $\alpha = 0.5$): $E°_{st} = -0.88$ V and $E°_c = -0.78$ V (vs SCE). The overall kinetics was controlled by electron transfer with competition between stepwise and concerted mechanisms.
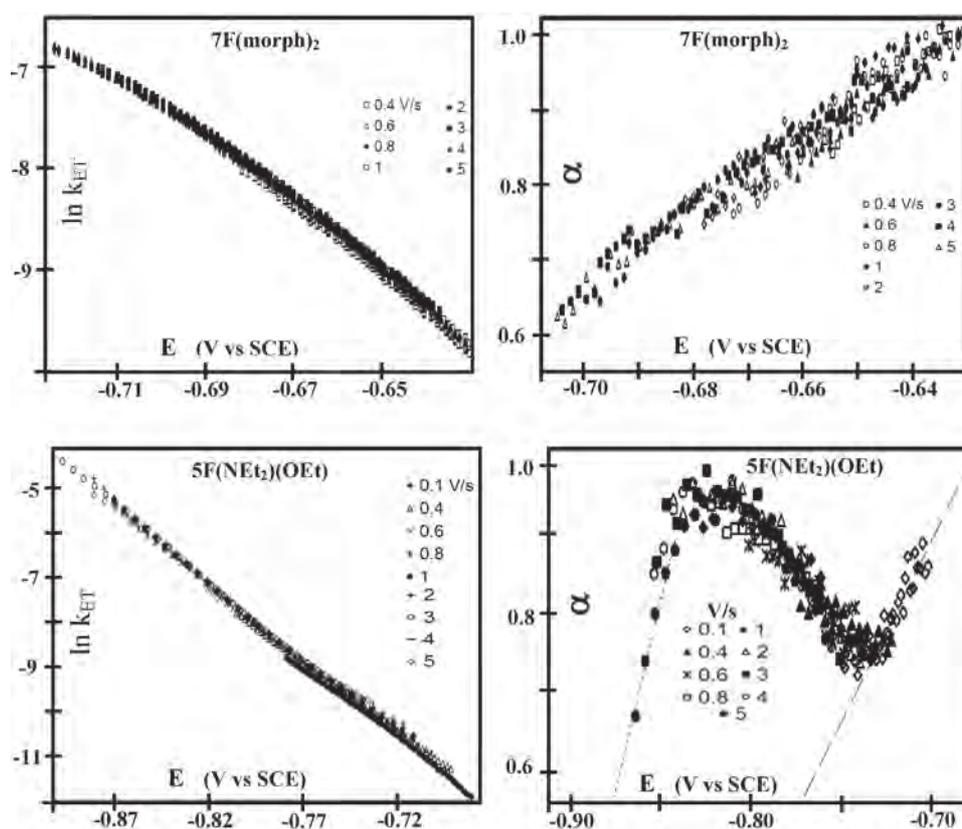
Fig. 7. Potential dependence of both the ln kET and electronic transfer coefficient α for 7F(morph)2 and 5F(NEt2)(OEt).

5. Conclusion

This study focused on the reduction of streptocyanines, a process assumed to obey the general mechanism: electron transfer followed by chemical reaction, proved to be a dimerization of the radical appearing at the electrode and this step can control the rate of the overall process for some streptocyanines. For others, the electron transfer is the limiting step.

Chain length influences both oxidation and reduction: the more the dye will be conjugated (lengthening the polyconjugated chain), the easier it will be to add or abstract one electron; but in reduction the amino end group has more influence than in oxidation as the electron density will be localized on odd carbons and so just in alpha position of the amino-end group although in oxidation the electron density is localized on even carbons and on beta position of the amino-end group.

For 5F(NEt$_2$)$_2$ the dimerization rate is about ten times lower than for 5F(morph)$_2$ and in the same range as for 7FN(Me$_2$)$_2$. Steric hindrance may explain this difference in reactivity. Similarly for 7F(morph)$_2$, the dimerization rate is very fast so electron transfer becomes the limiting step of the overall process.

The unpaired electron on 5F(NEt$_2$)(OEt) neutral radical is less delocalized on the dimerizing carbon center, than in the case of the 5C-streptocyanine neutral radical. C. Constentin and J. M. Savéant [32] showed that delocalized radicals may be endowed with quite significant activation barriers due to localization of the unpaired radical upon bond formation. The dimerization activation barrier increases as the thermodynamic driving force for forming the dimer decreases. Actually the dimerization of 5F(NEt$_2$)(OEt) neutral radical was very fast and kinetics controlled by electron transfer, with competition between the concerted and stepwise mechanisms.

The structures of 9C series are different, and the predominant limit form of the neutral radical formed is tertiary with a captodative effect when X = Cl, so, it has some degree of persistency. The k_χ is lower than in the other series. Dimerization was precluded in the case of 9F(morph)$_3$ as the radical was sterically hindered.

Quantum calculations using density functional theory (DFT) are undertaken in the aim to help understanding the observed difference in reactivity following the series and the substituents.

To check their potential for the treatment of malaria, antiplasmodial properties were previously evaluated [14]:

- 9F(morph)$_2$ for which E_{p1c} = −0.50 V is outside of the zone requisite to be activated by the redox machinery of the cell (−1.1 V to −0.7 V), is not active against *Plasmodium falciparum* nor toxic.
- 5F(NEt$_2$)(OEt) and in a lesser extent 7F(morph)$_2$, do not possess any biological activity as reduction immediately gave a neutral dimer.
- in the other cases the neutral radical formed could have time for instance to react with oxygen and generate oxidative stress.

Consequently, any clear relationship between bioactivity and electrochemical properties could be highlighted; several other parameters such as bioavailability, solubility, specific enzyme interactions and metabolism are also crucial for activity. Electrochemistry helps clarifying the mode of action of some of these drugs; nevertheless, many other important factors remain to be considered in the mechanistic aspects of their biological activity such as bioavailability, metabolism and specific enzyme interactions.

Appendix A. Supplementary data

Supplementary data associated with this article can be found, in the online version, at http://dx.doi.org/10.1016/j.electacta.2014.04.023.

References

[1] J. Fabian, H. Nakazumi, M. Matsuoka, Near-infrared absorbing dyes. Chem. Rev. 92 (1992) 1197–1226.

[2] A. Mishra, R.K. Behera, P.K. Behera, B.K. Mishra, G.B. Behera, Cyanines during the 1990: A review, Chem. Rev. 100 (2000) 1973–2011.

[3] W. West, Photographic Science and Engineering 18 (1974) 35.

[4] Z. Zhu., 35 Years Of Studies On The Chemistry Of Polymethine Cyanine, Dyes pigm. 27 (1995) 77–111.

[5] T. Ono, T. Yamaguchi, H. Arakawa, Study on dye-sensitized solar cell using novel infrared dye. Solar Energy Materials & Solar Cells 93 (2009) 831–835.

[6] H. Mustroph, M. Stollenwerk, V. Bressau, Current developments in optical data storage with organic dyes, Angew. Chem. Int. Ed. 45 (2006) 2016–2035.

[7] Z. Li, Z.H. Jin, K. Kasatani, H. Okamoto, S. Takenaka, Resonant enhancement of third-order nonlinear optical property in J-like aggregates of a cyanine, dye. Phys. Stat. Sol. (b) 242 (2005) 2107–2112.

[8] V. Guieu, C. Payrastre, Y. Madaule, S. Garcia-Alonso, P.G. Lacroix, K. Nakatani, Large quadratic nonlinear optical efficiencies in pseudosymmetric streptocyanine dyes, Chem. Mater. 18 (2006) 3674–3681.

[9] J. Malicka, I. Gryczynski, B.P. Maliwal, J. Fang, J.R. Lakowicz, Biopolymers, (Biospectroscopy) 72 (2003) 96.

[10] Y. Ye, S. Bloch, J. Kao, S. Achilefu, Multivalent carbocyanine molecular probes: Synthesis and applications, Bioconjug. Chem. 16 (2005) 51–61.

[11] K. Licha, C. Hessenius, A. Becker, P. Henklein, M. Bauer, S. Wisniewski, B. Wiedenmann, W. Semmler, Synthesis characterization, and biological properties of cyanine-labeled somatostatin analogues as receptor-targeted fluorescent probes, Bioconjug. Chem. 12 (2001) 44–50.

[12] I.G. Panova, N.P. Sharova, S.B. Dmitrieva, R.A. Poltavtseva, G.T. Sukhikh, A.S. Tatikolov, Use of a cyanine dye as a probe for albumin and collagen in the extracellular matrix, Anal. Biochem. 14 (2007) 183–189.

[13] K. Pudhom, K. Kasai, H. Terauchi, H. Inoue, M. Kaiser, R. Brun, M. Ihara, K. Takasu, Synthesis of three classes of rhodacyanine dyes and evaluation of their in vitro and in vivo antimalarial activity, Bioorg. Med. Chem. 14 (2006) 8550–8563.

[14] (a) M.-P. Maether, V. Bernat, M. Maturano, C. André-Barrès, S. Ladeira, A. Valentin, H. Vial, C. Payrastre, Synthesis and antiplasmodial activity of streptocyanine/peroxide and streptocyanine/4-aminoquinoline hybrid dyes, Organic and Biomolecular Chemistry 9 (2011) 7400–7410;
(b) M.P. Maether, D. Desoubzdanne, A. Izquierdo, V. Guieu, M. Maturano, C. André-Barrès, A. Valentin, V. Jullian, S. Chevalley, M. Maynadier, H. Vial, C. Payrastre, Synthesis and Antimalarial Properties of Streptocyanine Dyes, ChemMedChem 4 (2009) 1327–1332.

[15] E.A. Hillard, F. Caxico de Abreu, D.C.M. Ferreira, G. Jaouen, M.O.F. Goulart, C. Amatore, Electrochemical parameters and techniques in drug development, with an emphasis on quinones and related compounds, Chem. Comm. 261 (2008) 2612–2628.

[16] P.B. Gilman, R.L. Parton, J.R. Lenhard, U.S. Pat. Appl. Publ. (2006), US 20060099712 A1 20060511.

[17] F. Najjar, C. André-Barrès, M. Baltas, C. Lacaze-Dufaure, D.C. Magri, M.S. Workentin, T. Tzedakis, Electrochemical reduction of G3-factor endoperoxide and its methyl ether: Evidence for a competition between concerted and stepwise dissociative electron transfer, Chem. Eur. J. 13 (2007) 1174–1179.

[18] N. Obaya, C. Payrastre, Y. Madaule, Synthesis of new pentacarbon chain streptocyanines (pentamethinium salts), Tetrahedron 57 (2001) 9137–9147.

[19] A. Izquierdo, C. Payrastre, H. Gornitzka, Y. Madaule, Synthesis and reactivity of a new heptacarbon chain carboxonium salt - Access to a new class of streptocyanine dyes, Eur. J. Org. Chem. 13 (13) (2003) 2371–2374.

[20] A. Izquierdo, V. Guieu, H. Gornitzka, Y. Madaule, C. Payrastre, Synthesis and reactivity of a new nonacarbon chain carboxonium salt - Access to a new class of streptocyanine dyes, Eur. J. Org. Chem. 11 (2004) 2317–2320.

[21] V. Guieu, A. Izquierdo, S. Garcia-Alonso, C. André, Y. Madaule, C. Payrastre, Fluorescent streptocyanine dyes: Synthesis and photophysical properties - Synthesis of a new hemicarboxonium salt, Eur. J. Org. Chem. 5 (2007) 804–810.

[22] L. Nadjo, J.M. Savéant, Linear sweep voltammetry: kinetic control by charge transfer and/or secondary chemical reactions I. Formal kinetics, Electroanalytical Chemistry and Interfacial Electrochemistry 48 (1973) 113–145.

[23] C. P. Andrieux, J. M. Savéant, Electrochemical Reactions, In Investigations of Rates and Mechanism of Reactions, Techniques of Chemistry; Berbasconi, C. F., Ed.; Wiley: New York, 1986; vol. 6, Ch. VII, p 305-391.

[24] C. Imbeaux, J.M. Savéant, Convolutive potential sweep voltammetry. I. Introduction. J. Electroanal. Chem. Interfacial Electrochem. 44 (1973) 169–187.

[25] J.M. Savéant, D. Tessier, Convolution potential sweep voltammetry. Part IV. Homogeneous follow-up chemical reactions, J. Electroanal. Chem. Interfacial Electrochem. 61 (1975) 251–262.

[26] C.P. Andrieux, L. Nadjo, J.M. Savéant Electrodimerization, V.I.I Electrode and solution electron tranfers in the radical-substrate coupling mechanism. Discriminative criteria from the other mechanisms in voltammetric studies, J. Electroanal. Chem. Interfacial Electrochem. 42 (1973) 223–242.

[27] A. Muthukrishnan, M.V. Sangaranarayanan, Analysis of C-F bond cleavages in methylfluorobenzoates.- Fragmentation and dimerization of anion radicals using convolution potential sweep voltammetry, Electrochimica Acta 55 (2010) 1664–1669.

[28] J.M. Savéant, D. Tessier, Non-Volmerian Charge Transfers Associated with Follow-up Chemical reactions. A convolution Potential Sweep Voltammetric Study of Benzaldehyde Reduction in Ethanol, The Journal of Physical Chemistry 82 (15) (1978) 1723–1727.

[29] H.K. Hall, Jr. Correlation of the base strengths of amines, J. A.m. Chem. Soc. 79 (1957) 5441.

[30] L. Nadjo, J.M. Savéant, D. Tessier, X.I. Electrodimerization, Coupling mechanism of an activated olefin: p- methylbenzylidene-malononitrile as studied by convolution potential sweep voltammetry, J. Electroanal. Chem. 64 (1975) 143–154.

[31] C. André-Barrès, F. Najjar, M.P. Maether, C. Payrastre, P. Lavedan, T. Tzedakis, J. Comparison of diffusivities data of streptocyanine dyes by electrochemical and NMR-DOSY methods, Electroanalytical Chem. 686 (2012) 54–57.

[32] C. Costentin, J.M. Savéant, Origin of activation barriers in the dimerization of neutral radicals: A nonperfect synchronization effect? J, Phys. Chem A 109 (2005) 4125–4132.